Partial wave analysis of $K^*\bar{K}$ events in GlueX

Sebastian Cole

Arizona State University

7/2/2021

Table of contents

Table of Contents

Thomas Jefferson national accelerator facility

Jefferson lab

Located in Newport News, Virginia, Jefferson Lab is home to an electron accelerator that support four experimental halls [1].

The continuous electron beam accelerator facility

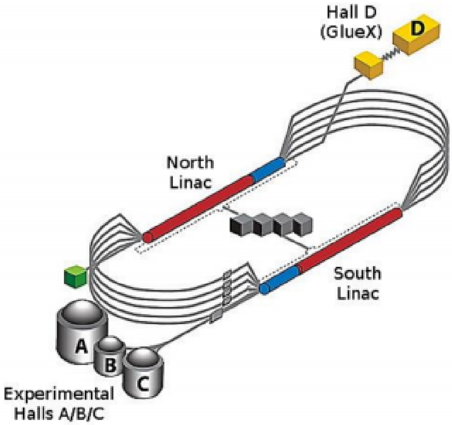

Continuous electron beam accelerator facility (CEBAF)

CEBAF consists of two linacs making an ~ 1.4 km racetrack shaped, electron accelerator capable of producing an ~ 12 GeV electron beam.

The GlueX Bremsstrahlung photon beamline

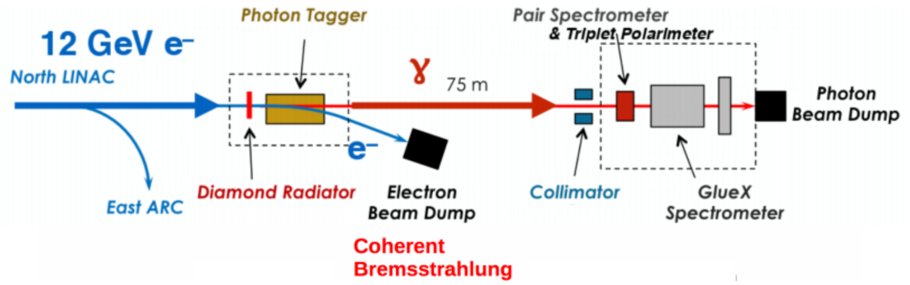

Beamline overview

The GlueX beamline consists of a thin diamond radiator held by a goniometer from which a polarized photon beam is created through the bremsstrahlung process. Scintillating detectors are used to reconstruct the photon beam energies and a silicon strip detector is used to determine photon beam polarization [2].

The GlueX spectrometer

GlueX spectrometer overview

The GlueX spectrometer consists of six sub-detectors. A cryogenic hydrogen target is inserted into a tracking volume such that it is surrounded by the central drift chamber, the barrel calorimeter, and a superconducting solenoid. The forward drift chamber caps the downstream end of the tracking volume. The forward calorimeter and time of flight planar detectors cover the downstream end of the hall [3].

Goals of the GlueX experiment

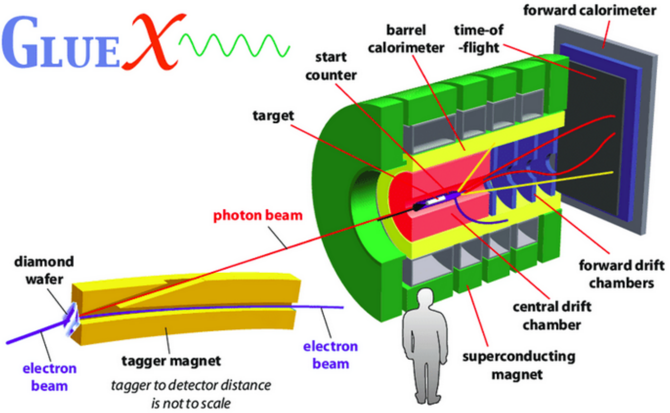

Goals

1 Map the light meson spectrum.

2 Find hybrid mesons with exotic quantum numbers [4].

Table of Contents

The Standard Model[5]

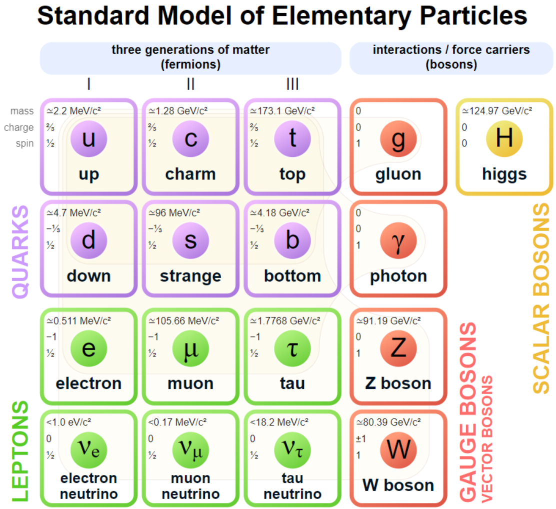

Hadrons[6]

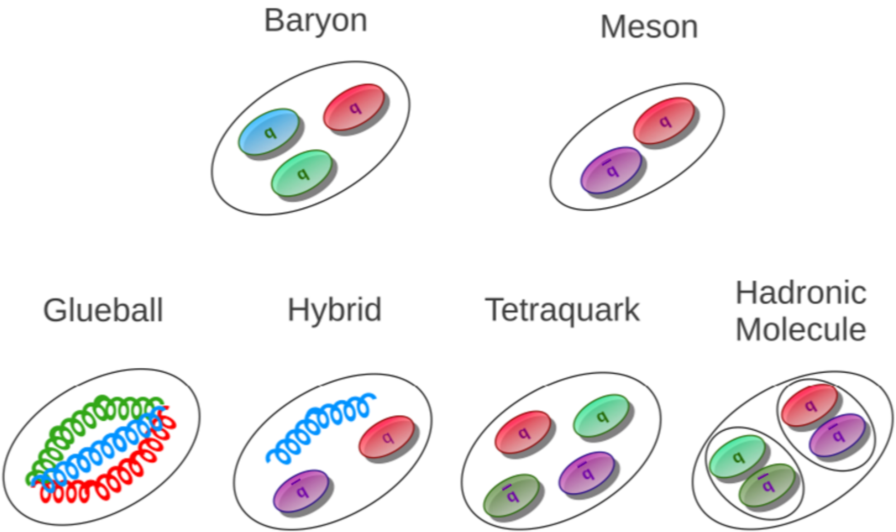
Baryon
Meson
Glueball
Hybrid
Tetraquark
Hadronic
Molecule

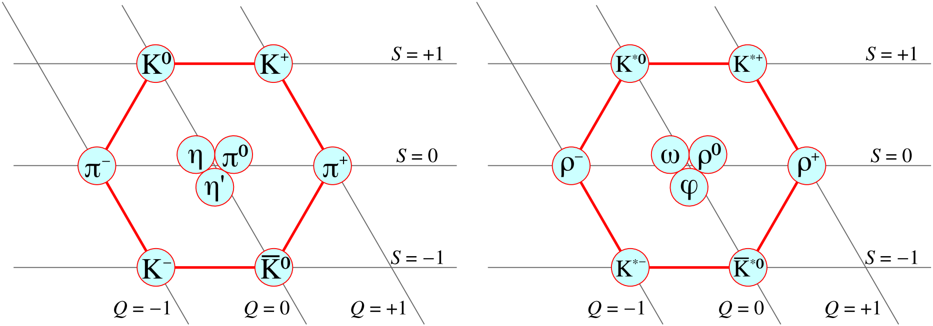

Murray Gell-Mann, Yuval Ne'eman, George Zweig, and Kazuhiko Nishijima

- Gell-Mann and Nishijima -*strangeness* to describe long lived particles.
- Gell-Mann and Ne'eman - *the eightfold way* in 1961.
- Gell-Mann and Zweig - *multiplets* using electrical charge and strangeness [7] [8].

Constituent quark model

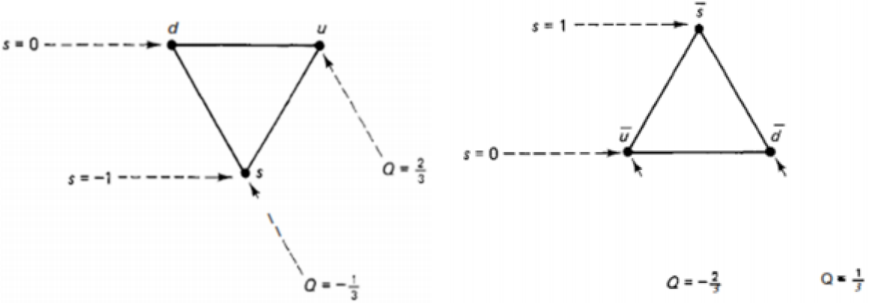

Murray Gell-Mann and George Zweig

- A result of explaining ϕ meson preferential decay to two kaons.
- Gell-Mann and Zweig - *quarks* are the building blocks of hadrons[a].
- Quarks - spin-$\frac{1}{2}$ particles consisting of *up*, *down*, and *strange*.
- No free quarks, *confined* to hadrons.
- Restricts possible J^{PC} quantum numbers [9].

[a] Zweig called them *aces*.

Mesons in constituent quark model

J^{PC} quantum numbers

S - Intrinsic spin
L - Orbital angular momentum
J - Total angular momentum
$J = L \oplus S$
P - Parity $P = (-1)^{L+1}$
C - Charge conjugation
$C = (-1)^{L+S}$

Possible J^{PC}

According to the rules of the constituent quark model, can only have radial and orbital excitations. For meson states, this means only:

$$0^{-+}, 0^{++}, 1^{--}, 1^{+-}, 2^{--}, 2^{-+}, 2^{++}, 3^{--}, \ldots$$

J^{PC} quantum numbers are allowed, leaving:

$$0^{--}, 0^{+-}, 1^{-+}, 2^{+-}, 3^{-+}, \ldots$$

as forbidden by the constituent quark model.

S	L	J	P	C	J^{PC}	Meson type
0	0	0	$-$	$+$	0^{-+}	pseudoscalar
1	0	0	$-$	$-$	1^{--}	vector
0	1	1	$+$	$-$	1^{+-}	pseudo-vector
1	1	0	$+$	$+$	0^{++}	scalar
1	1	1	$+$	$+$	1^{++}	axial vector
1	1	2	$+$	$+$	2^{++}	tensor

Hadrons[6]

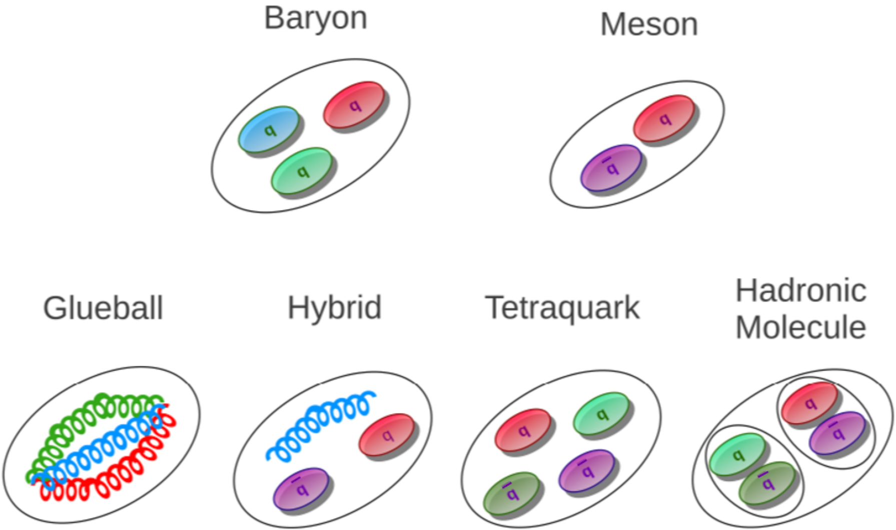
Baryon
Meson
Glueball
Hybrid
Tetraquark
Hadronic Molecule

HadSpec predictions

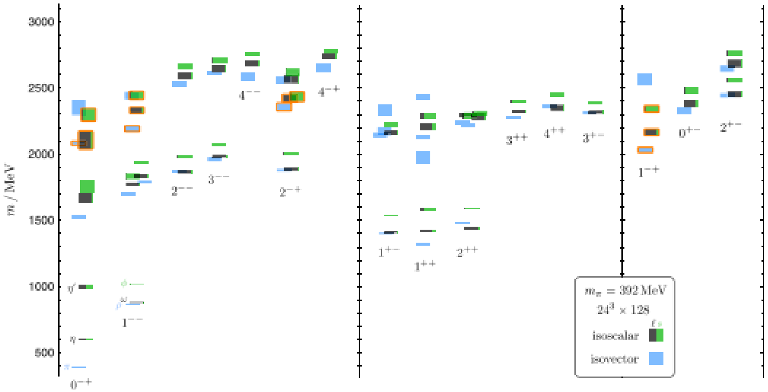

Interpretation

J^- on left, J^+ middle, and exotic quantum numbers right. Hybrid mesons are marked in orange and possible strange quark contributions are marked in green [10].

Light meson spectrum

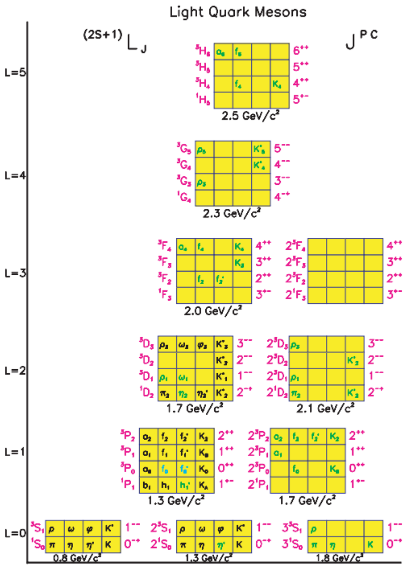

Orbital and radial excitations

Orbital excitations are displayed by the y-axis and radial excitations are shown on the x-axis. The figure displays spectroscopic notation $^{2\mathbf{S}+1}\mathbf{L_J}$, J^{PC} of the nonet, and the name of the states. If shown in black, the state is well established. If you include exotic quantum numbers, this adds many more mesons are added [**TDR**].

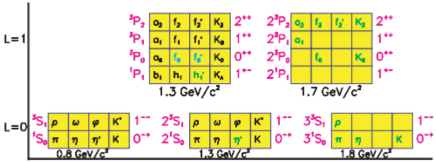

Table of Contents

The E/ι puzzle

Pseudoscalar in $\bar{p}p$ annihilation at rest

In 1963, peak at 1425 MeV seen in $K\bar{K}\pi$ mass spectrum with $J^{PC} = 0^{-+}$ dubbed E meson [11].

E and ι separate particles

Different quantum numbers for different production mechanisms from spin-parity analysis, specifically the E meson 0^{-+} and the ι meson 1^{++} [11].

The 1998 PDG

The 1998 PDG reports an axial vector $f_1(1420)$ and pseudoscalar $\eta(1440)$ as the ι and E, respectively [12].

J/ψ decays at MARKIII

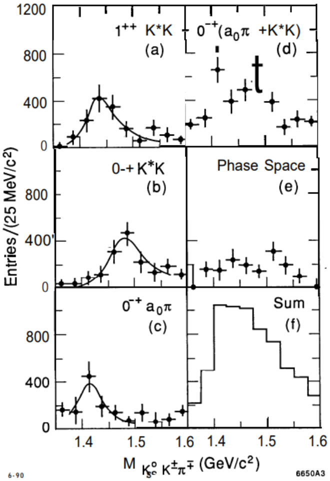

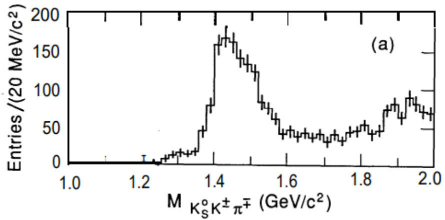

Two psuedoscalars in $K\bar{K}\pi$

Reported psuedoscalars at $1416\ \mathrm{MeV}$ and $1490\ \mathrm{MeV}$ decaying $a_0(980)\pi$ and $K^*(892)\bar{K}$ in J/ψ decays [13]. Confirmed by DM2 experiment [14].

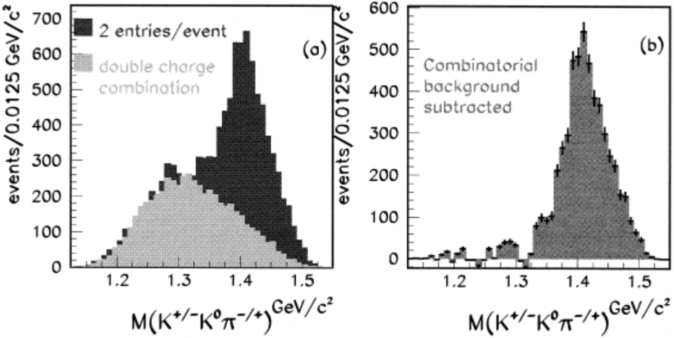

OBELIX evidence of two psuedoscalar states in $1.4 - 1.5$ GeV region

In $p\bar{p}$ annihilation at rest, OBELIX shows evidence of two psuedoscalar mesons decaying $K\bar{K}\pi$ in the mass region of interest [11].

$\gamma\gamma$ collisions in L3

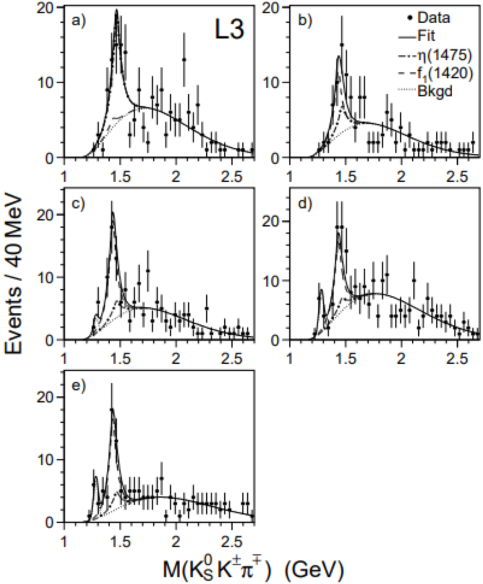

Evidence of $\eta(1475)$ in $\gamma\gamma$ collisions

The L3 collaboration shows evidence of $\eta(1475)$ in $\gamma\gamma$ collisions, but not the $\eta(1405)$. This supports the argument that $\eta(1405)$ consists only of gluonic content [15].

E852 at Brookhaven PWA results

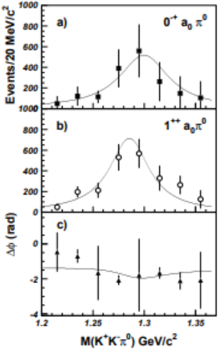

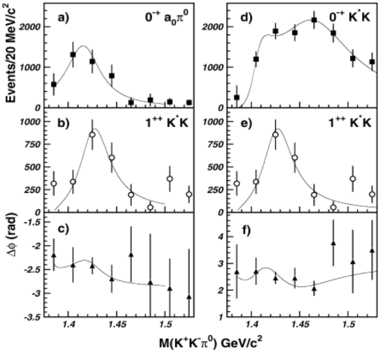

PWA of $K^+K^-\pi^0$

Evidence of $\eta(1295)$ and $f_1(1285)$ decay $a_0(980)\pi^0$ left. Evidence of $\eta(1416)$ decay $a_0(980)\pi^0$ and $K^*\bar{K}$, and $\eta(1485)$ and $f_1(1420)$ decay $K^*\bar{K}$ right [16].

Interpretation of previous results

The $\eta(1295)$ and $\eta(1475)$ pseudoscalars

The existence of the $\eta(1295)$ seen in $\pi^- p$, J/ψ decays, and B meson decays is debated. Assuming the $\eta(1295)$ exists, then it may be the first radial excitation of η and the $\eta(1475)$ is the first radial excitation of η'. The $\eta(1475)$ isoscalar would be the $s\bar{s}$ contribution to the 0^{-+} nonet.

The $\eta(1405)$ pseudoscalar

If two pseudoscalar mesons exist in the $1400\ \mathrm{MeV}$ region, the $\eta(1405)$ might be something other than a meson, specifically 0^{-+} glueball. This is supported by the fact that it is not seen in $\gamma\gamma$ collisions in L3. This is not supported by lattice gauge theory, but is by the flux tube model [17].

Motivation for the analysis of $\gamma p \to p K^+ K^- \gamma\gamma$ events

Analysis of $X \to K^* \bar{K}$

1. Do two psuedoscalar mesons exist in the 1400 MeV region seen in production mechanisms: $\pi^- p$, radiative $J/\psi(1S)$ decay, and $\bar{p}p$ annihilation at rest?
2. What additional states can be found in the mass range used in this analysis?

We perform a partial wave analysis in search of mesons decaying $K^* \bar{K}$ to answer these questions [**TDR**].

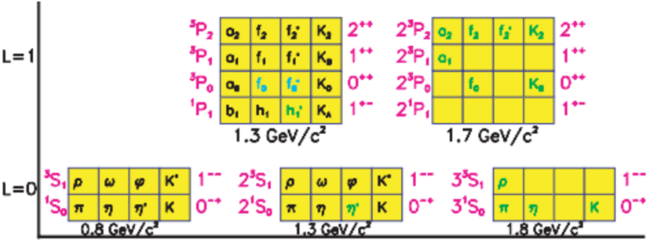

Table of Contents

Reconstruction

Charged particles

Charged particles are reconstructed using a helical fit of their points of detection in the CDC and other detectors. This fit is dependent on the assumed identification of a particle. If the fit converges, the identification hypothesis and its respective kinematic information is kept.

Neutral paritcles

Neutral particles are reconstructed using their electromagnetic showers in BCAL and FCAL.

Events

Events are produced based on combinations of the charged tracks and neutrals, coupled with the beam photons in time with the event. This is a combinatorial problem since the selection of charged and neutral particles comes from a set larger than what is required for a reaction.

Beam photons

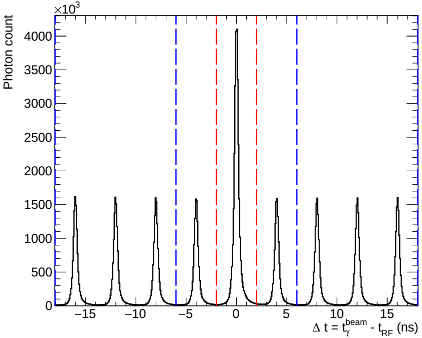

Beam photon selection

Beam photons in time with detected events fall between -2.004 and 2.004 ns, surrounded by side-band peaks from out of time beam photons. One photon is selected per event with signal photons recieving a weight of 1 and side-band photons are given a weight of $-f/N_a$, where N_a is the number of accidental side-bands used and f is a correction factor. For PWA, photons with energies from $8.2 - 8.8$ GeV are selected.

Selection of tracks in time with beam photons

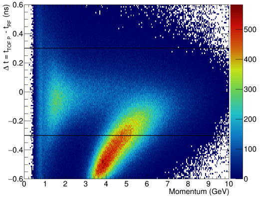

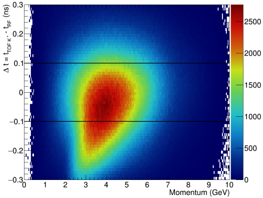

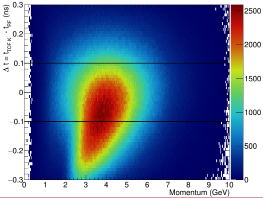

Δt for a charged tracks or neutrals

The time for an event at the vertex is determined by propagating back to the vertex within the target volume. From the tracking reconstruction, it is possible to determine the time an event occurs for each particle hypothesis. The distribution is centered over zero for the correct particle identification.

Detector	Δt_p (ns)	$\Delta t_{K^\pm}$ (ns)	Δt_γ (ns)
BCAL	± 0.5	± 0.2	± 2.0
FCAL	± 1.0	± 0.5	± 2.0
TOF	± 0.3	± 0.15	NA
ST	None	None	NA
NULL	None	None	NA

Event selection

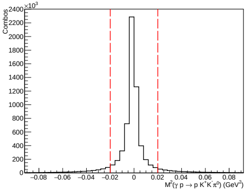

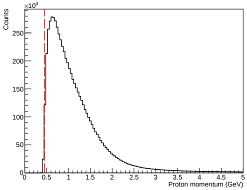

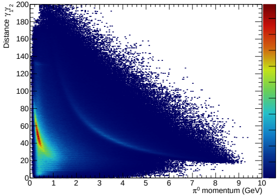

Removal conditions
$\chi^2/n.d.f. > 5$
$\theta_\gamma < 1.5°$
$10.3° < \theta_\gamma < 11.5°$
$E_{BCAL}^{min} < 0.05$ GeV
Shower quality FCAL < 0.5
$d_{\gamma_1,\gamma_2} < 12.5$ cm
$MM^2 > 0.2$ GeV
$p_p^{recoil} < 0.45$ GeV
52 cm $< z_{vertex} > 78$ cm
$r_{vertex} > 1$ cm

Selection of combination

Combination with best $\chi^2/n.d.f.$ from kinematic fit is selected.

Kinematic fitting

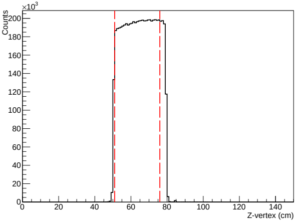

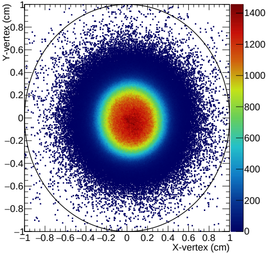

Kinematic fitter

A four-momentum and vertex kinematic fit is performed through a χ^2 minimization, determined by

$$\chi^2 = (\boldsymbol{\eta_0} - \boldsymbol{\eta_f})^T \mathbf{G_y} (\boldsymbol{\eta_0} - \boldsymbol{\eta_f})$$

where η_0 is the vector of the quantity values before the fit, η_f is the vector of the quantity values after the fit, and G_y is the inverse of the covariance matrix for those quantities.

$\pi^0 \rightarrow \gamma\gamma$

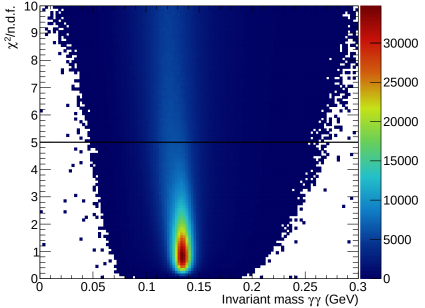

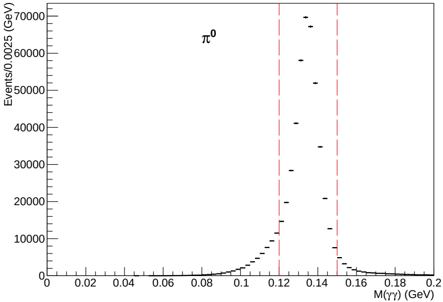

π^0 selection

From Gaussian with third degree polynomial fit, π^0 mesons is selected using 2σ from center, $0.12 - 0.15$ GeV as shown by dashed lines.

$K^*(892) \to K\pi^0$

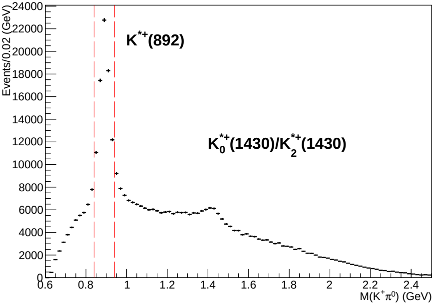

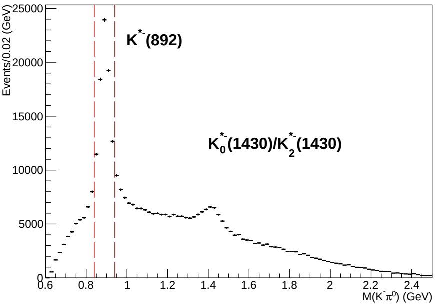

$K^*(892)$ selection

From Gaussian with third degree polynomial fit, $K^*(892)$ mesons is selected using 2σ from center, $0.84 - 0.94$ GeV as shown by dashed lines.

Excited K^*

A peak for excited K^* mesons near ~ 1.4 GeV is visible. This may include $K_1^*(1410)$, predicted to be an η_1' hybrid meson candidate decay product.

$X \to K^{*\pm}(892)K^{\mp}$

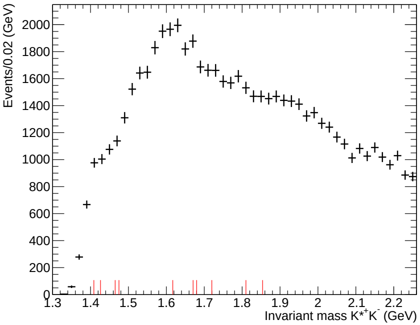

Possible meson states

Visible peak near ~ 1.4 GeV for both distributions. This is consistent with $\eta(1405)$, $f_1(1420)$, $\rho(1450)$, and $\eta(1475)$. Difficult to make any other conclusions for higher mass peaks without PWA.

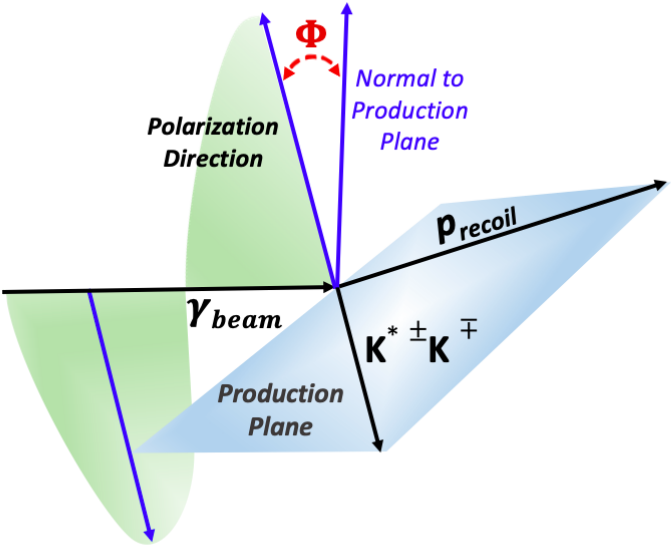
Φ
Normal to
Production
Plane
Polarization
Direction
p_{recoil}
γ_{beam}
$K^{*\pm}K^{\mp}$
Production
Plane

Angular distributions cont.

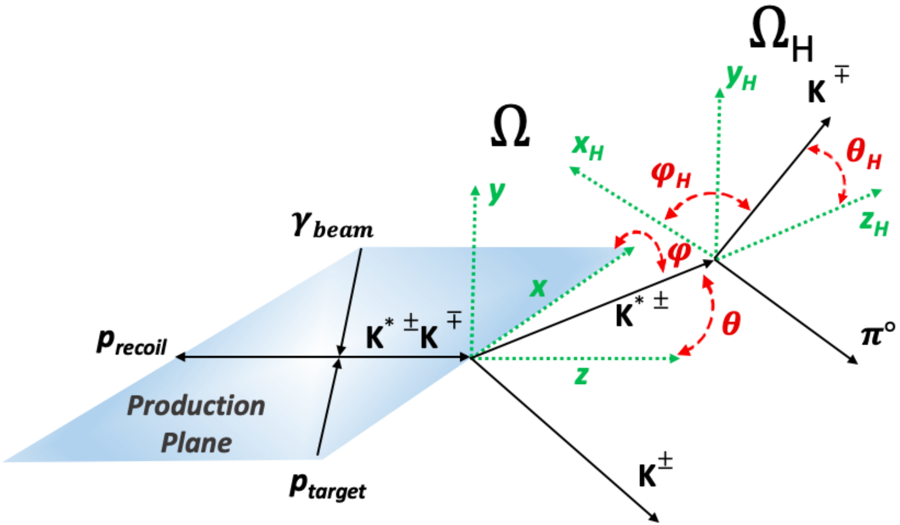

$K^*\bar{K}$ Monte Carlo

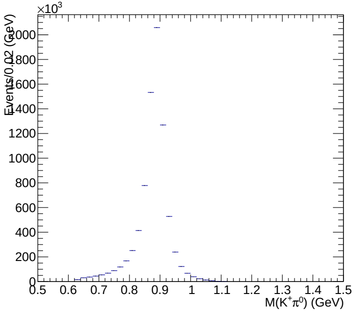

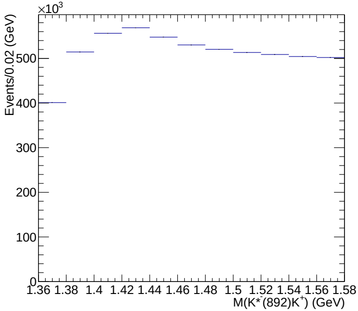

Generator and simulation

- Randomly generate samples of $K^*\bar{K}$ isotropically through phase space.
- Pass generated events through simulation of GlueX spectrometer.
- Flat incident photon beam energy from $8.2 - 8.6$ GeV.
- The K^* mass distribution is given a Breit-Wigner shape.
- t-slope$= 1.3/\text{GeV}^2$

$K^*\bar{K}$ Monte Carlo cont.

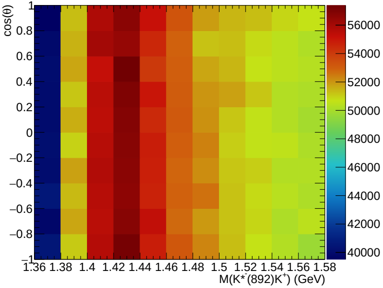

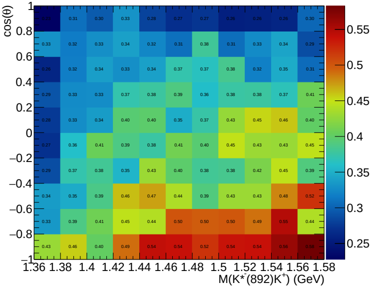

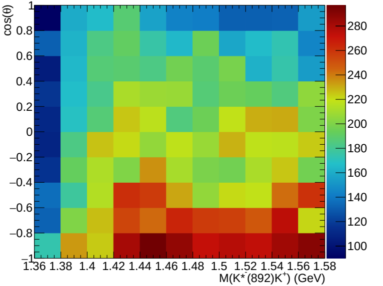

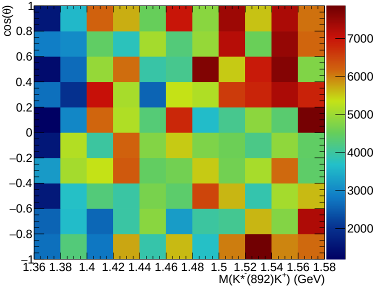

Partial wave analysis

Intensity function in reflectivity basis requiring positive reflectivity

Obtain fit parameters $[J_i^P]_{m,k}^{(\epsilon)}$ for different wave contributions with fits to the angular distributions using the intensity function:

$$I(\Omega, \Omega_H, \Phi) = 2\kappa \sum_k [(1 - P_\gamma)[|\sum_{i_N,m} [J_i^N]_{m,k}^{(+)} Im(Z)|^2 + |\sum_{i_U,m} [J_i^U]_{m,k}^{(+)} Re(Z)|^2] + (1 + P_\gamma)[|\sum_{i_U,m} [J_i^U]_{m,k}^{(+)} Im(Z)|^2 + |\sum_{i_N,m} [J_i^N]_{m,k}^{(+)} Re(Z)|^2]],$$

where

$$Z = e^{-i\Phi} \sum_{m_2''} \sum_{m'} D_{mm'}^{J_i *}(\Omega) \langle Jm' | j_1 m_1 j_2 m_2'' \rangle D_{m_2'',m_2}^{j_2 *}(\Omega_H) [18].$$

Partial wave analysis cont.

Quantum numbers

- J and M are the total angular momentum and spin projection of the meson resonance.
- L and m_L are the orbital angular momentum and spin projection of the meson resonance's decay, for which a P
- S and m_S are the spin and spin projection of the vector meson.

Wave conditions

- Require positive reflectivity.
- $J = 0$, 1, and 2 for spin projections M from $-J$ to J are included for the four coherent sums.
- To reduce fit parameters, the orbital angular momentum of the decay L is restricted to P, S, and D waves for each J, respectively.
- To conserve total angular momentum $M = m_L + m_S$.

J	M	L	m_L	S	m_S
0	0	1	-1	1	1
0	0	1	0	1	0
0	0	1	1	1	-1
1	-1	0	0	1	-1
1	0	0	0	1	0
1	1	0	0	1	1
2	-2	2	-2	1	0
2	-2	2	-1	1	-1
2	-1	2	-2	1	1
2	-1	2	-1	1	0
2	-1	2	0	1	-1
2	0	2	-1	1	1
2	0	2	0	1	0
2	0	2	1	1	-1
2	1	2	0	1	1
2	1	2	1	1	0
2	1	2	2	1	-1
2	2	2	1	1	1
2	2	2	2	1	0

Unbinned fitting

Unbinned extended maximum likelihood fit

The likelihood is defined in terms of the intensity as

$$-2\ln\mathcal{L} = 2\mu - 2\sum_{i=1}^{n}\ln I(\Omega_i) + \text{constant}.$$

where 2μ is a normalization determined by Monte Carlo integration, the sum is produced from the data, and the constant is ignored since it has no effect on minimization. The expected number of events μ as a function of the angular distribution

$$\mu = \int d\Omega I(\Omega)\eta(\Omega),$$

where η efficiency correction term.

Fit constraints

Between coherent sums

- Four fit parameters, two $[J_i^N]^{(+)}$ and two $[J_i^U]^{(+)}$.
- Identical fit parameters constrained.

Simultaneous fit

- Data broken into eight subsets with meson resonance deacys $K^{*+}K^-$ and $K^{*-}K^+$ for each polarization.
- Identical fit parameters between the eight subsets are constrained.
- $J = 0$ with P-wave forced to real.
- Number of fit parameters reduced from 192 to 10.
- Simultaneous fit between these subsets of the data reduces statistical uncertainty.

PWA fit results for

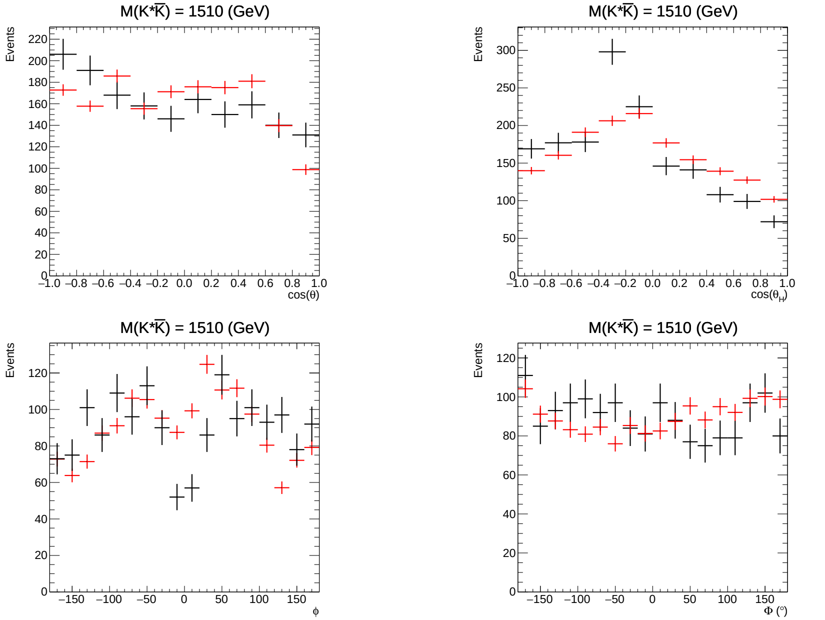

Uncertainty determination

Fit

Plot $\cos\theta$, $\cos\theta_H$, ϕ, and Φ of PWA fit results for all subsets. Fit histograms to the data. Extract fractional uncertainties of the coefficients.

$$h_{tot} = a_0 h_0 + a_1 h_1 + a_2 h_2 + C$$

$$\sigma_m = \frac{\sigma_{a_n}}{a_n} m$$

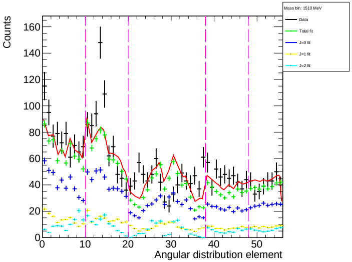

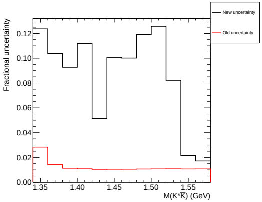

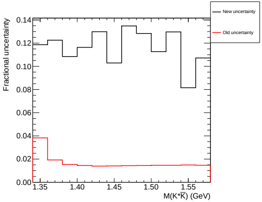

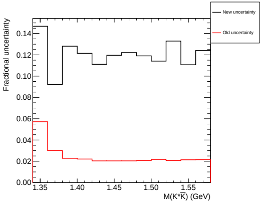

$K^* \bar{K}$ invariant mass for each total angular momentum

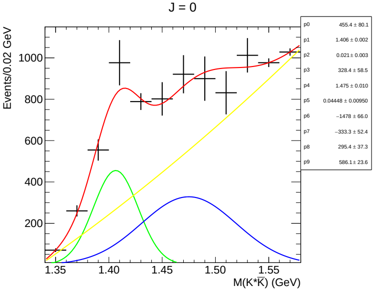

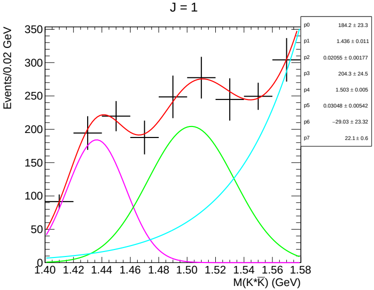

Results of PWA

- $J = 0$: Evidence of $\eta(1405)$ and $\eta(1475)$.
- $J = 1$: Evidence of $f_1(1420)$ and $f_1(1510)$.
- $J = 2$: Evidence of $f_2(1430)$ and $f_2(1530)$.

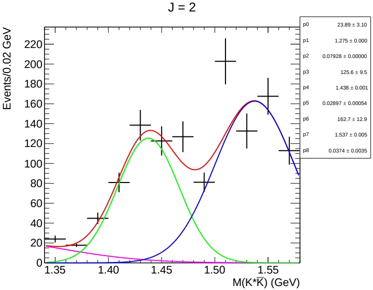

Invariant mass fit results

Results of PWA

- $J = 0$: Evidence of $\eta(1405)$ and $\eta(1475)$.
- $J = 1$: Evidence of $f_1(1420)$ and $f_1(1510)$.
- $J = 2$: Evidence of $f_2(1430)$ and $f_2(1530)$.

J	PID	PDG center (MeV)	PDG width (MeV)	Fit center (MeV)	Fit width (MeV)
0	$\eta(1405)$	1408.8 ± 2.0	50.1 ± 2.6	1406 ± 2	49.46 ± 7.07
0	$\eta(1475)$	1475 ± 4	90 ± 9	1475 ± 10	105.8 ± 224
1	$f_1(1420)$	1426.3 ± 0.9	54.5 ± 2.6	1436 ± 11	48.40 ± 4.17
1	$f_1(1510)$	1518 ± 5	73 ± 25	1503 ± 5	71.78 ± 12.76
2	$f_2(1430)$	$\sim$1430	NA	1438 ± 1	68.22 ± 1.27
2	$f_2(1525)$	1517.4 ± 2.5	86 ± 5	1537 ± 5	88.10 ± 8.24

Table of Contents

Motivation revisited

Analysis of $X \to K^* \bar{K}$

1 Do two psuedoscalar mesons exist in the $1400\ \mathrm{MeV}$ region seen in production mechanisms: $\pi^- p$, radiative $J/\psi(1S)$ decay, and $\bar{p}p$ annihilation at rest?

2 What additional states can be found in the mass range used in this analysis [**TDR**]?

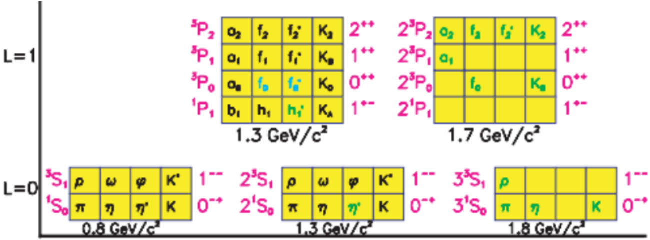

$J = 0$ states

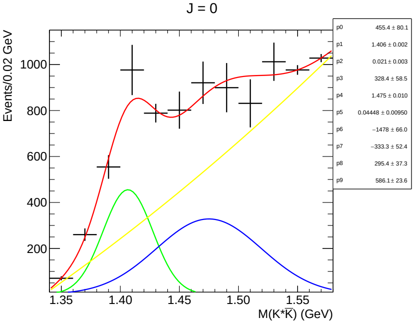

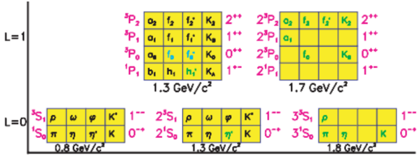

J=0 results

- Two pseudoscalar mesons in $1400\ \mathrm{MeV}$ mass region.
- Is the $\eta(1405)$ or the $\eta(1475)$ the $s\bar{s}$ contribution to the first radially excited pseudoscalar nonet?
- What about the glueball state explanation since this is produced in photoproduction? Is this an example of Pomeron exchange [**TDR**]?

$J = 1$ states

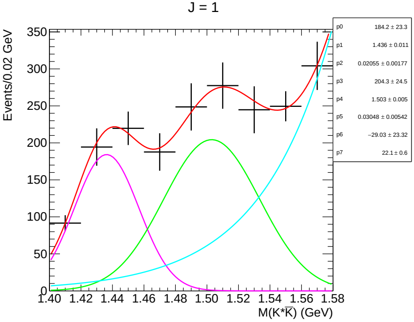

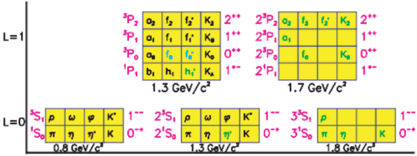

J=1 results

- Two axial vector mesons in $1400 - 1500\ \mathrm{MeV}$ mass region.
- Is the $f_1(1420)$ or $f_1(1510)$ the $s\bar{s}$ contribution to the axial vector meson nonet?
- Can the $f_1(1510)$ be firmly established [**TDR**]?

$J = 2$ states

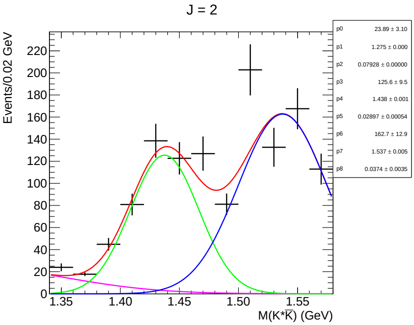

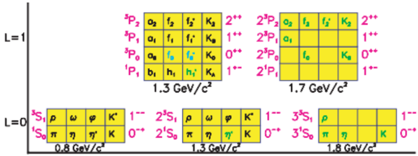

J=2 results

- Two tensor mesons in $1400 - 1500$ MeV mass region.
- Can we establish $f_2(1430)$ in a new decay mode?
- If the $f_2(1430)$ exist, is it or the $f_2'(1525)$ the $s\bar{s}$ contribution to the tensor meson nonet [**TDR**]?

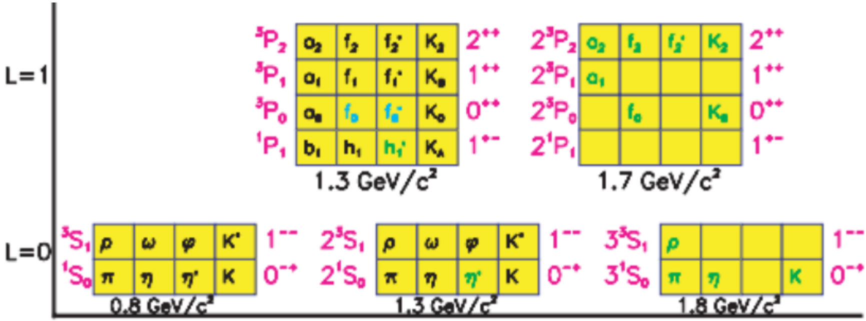

How can this be resolved?

The K_L would help establish the $s\bar{s}$ meson contributions to the pseudoscalar, axial vector, and tensor meson nonets. The extraneous states would require glueball, hadronic molecule, or tetraquark explanations [**TDR**].

Discussion

Completed

- Multiple states identified in the $1400 - 1500\ \mathrm{MeV}$ mass region.
- These states are consistent with past results.
- Consistent pattern between the three nonets.

Future

- Future work will move up the $K^*\bar{K}$ mass spectrum.
- Look at the other meson resonance decays, $a_0\pi^0$ and $K^+K^-\pi^0$.
- Can the group provide evidence of the η_1' hybrid meson candidate?

LQCD hybrid predictions

Masses

0^{+-} ~2.3 – 2.5 GeV
1^{-+} ~2.0 – 2.4 GeV
2^{+-} ~2.4 – 2.6 GeV

Widths

Γ ~0.1 – 0.5 GeV
$\Gamma_{1^{-+}} \approx \Gamma_{2^{+-}} < \Gamma_{0^{+-}}$

J^{PC}	Particle	Decays
0^{+-}	b_0	$\pi(1300)\pi,\ h_1\pi,\ f_1\rho,\ b_1\eta$
	h_0	$b_1\pi,\ h_1\eta$
	h_0'	$K_1(1270)\bar{K},\ K(1410)\bar{K},\ h_1\eta$
1^{-+}	π_1	$\rho\pi,\ b_1\pi,\ f_1\pi,\ \eta\pi,\ \eta'\pi,\ a_1\eta$
	η_1	$f_1\eta,\ a_2\pi,\ f_1\eta,\ \eta'\eta,\ \pi(1300)\pi,\ a_1\pi$
	η_1'	$K^*\bar{K},\ K(1270)\bar{K},\ K(1410)\bar{K},\ \eta'\eta$
2^{+-}	b_2	$\omega\pi,\ a_2\pi,\ \rho\eta,\ f_1\rho,\ a_1\pi,\ h_1\pi,\ b_1\eta$
	h_2	$\rho\pi,\ b_1\pi,\ \omega\eta,\ f_1\omega$
	h_2'	$K_1(1270)\bar{K},\ K(1410)\bar{K},\ K_2\bar{K},\ \phi\eta,\ f_1\phi$

[1] C. Meyer *et al.*, [arXiv:1004.551].

Partial wave analysis

The intensity of a meson states production is defined in terms of the differential cross section:

$$I(\Omega, \Omega_H, \Phi) \equiv \frac{d\sigma}{dt\ dm_{K^*\bar{K}}\ d\Omega\ d\Omega_H\ d\Phi}.$$

In terms of phase rotated decay amplitudes $\tilde{A}_\pm(\Omega, \Omega_H, \Phi) = e^{\mp i\Phi} A_\pm(\Omega, \Omega_H, \Phi)$ in a reflectivity basis

$$I(\Omega, \Omega_H, \Phi) = 2\kappa \sum_k [(1-P_\gamma)[|\sum_{i_N,m}[J_i^N]^{(+)}_{m,k} Im(Z) + \sum_{i_U,m}[J_i^U]^{(-)}_{m,k} Im(Z)|^2$$
$$+|\sum_{i_N,m}[J_i^N]^{(-)}_{m,k} Re(Z) + \sum_{i_U,m}[J_i^U]^{(+)}_{m,k} Re(Z)|^2] + (1+P_\gamma)[|\sum_{i_N,m}[J_i^N]^{(-)}_{m,k} Im(Z)$$
$$+\sum_{i_U,m}[J_i^U]^{(+)}_{m,k} Im(Z)|^2 + |\sum_{i_N,m}[J_i^N]^{(+)}_{m,k} Re(Z) + \sum_{i_U,m}[J_i^U]^{(-)}_{m,k} Re(Z)|^2]].$$

$$A_\lambda = \sum_i \sum_m T^i_{\lambda,m} \sum_\lambda D^{J_i *}_{m,\lambda}(\Omega) F^i_\lambda D^{1*}_{m,\lambda}(\Omega_H), \tag{1}$$

Unbinned fitting

Unbinned extended maximum likelihood fit

The expected number of events μ as a function of the angular distribution

$$\mu = \int d\Omega I(\Omega)\eta(\Omega),$$

where η efficiency correction term.

Likelihood

The likelihood is defined in terms of the intensity as

$$\mathcal{L} = \frac{e^{-\mu}}{n!}\prod_{i=1}^{n} I(\Omega_i),$$

which by Sterling is

$$-2\ln\mathcal{L} = 2\mu - 2\sum_{i=1}^{n}\ln I(\Omega_i) + \text{constant}$$

where 2μ is a normalization determined by Monte Carlo integration, the sum is produced from the data, and the constant is ignored since it has no effect on minimization.

Why a polarized photon beam?

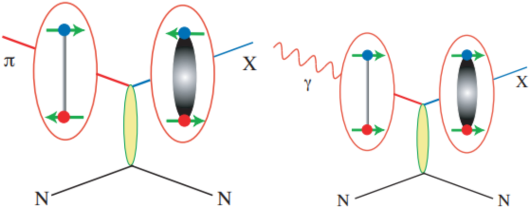

Photon beam

Pion beam has anti-aligned spins $(S = 0)$, while photon beam is a virtual meson with aligned spins $(S = 1)$. Starting with $J^{PC} = 1^{--}$ allows for mesons with exotic quantum numbers that are suppressed by a pion beam.

Linear polarization

Linearly polarized states are eigenstates of parity. Orientation of linear-polarization maps onto the naturality of the exchange particle (Natural: $J^P = 0^+, 1^-, 2^+, ...$ and Unnatural: $J^P = 0^-, 1^+, 2^-, ...$) [**GlueX˙TDR**].

[1] F. Barbosa *et al.* (GlueX)

$\phi\pi^0$ decay in Serpukhov data

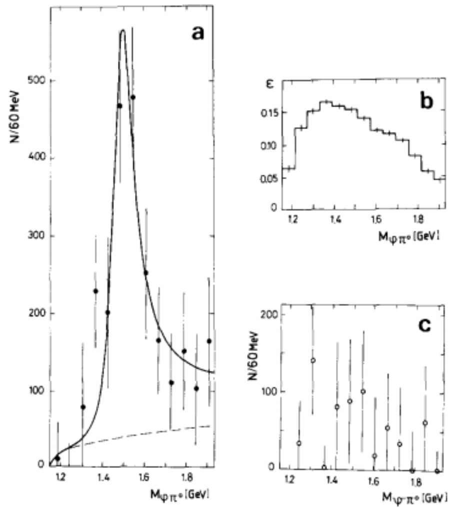

Serpukhov analysis

The Serpukhov figure shows the (a) $C(1480)$ invariant mass distribution from fits the ϕ distribution to remove background. The (b) acceptance for $\phi\pi^0$ and a (c) false "ϕ"π^0 from mis-identification of kaons are also shown. The $C(1480)$ is not seen in $\bar{p}p$ experiment and not seen by E852 [**Serpukhov**]. The PDG reports the $C(1480)$ as the $\rho(1570)$ seen in $\eta\rho \to \eta\pi\pi$.

[1] S. Bityukov *et al.* (SERPUKHOV), Phys. Lett. **B188**, 383 (1987).

$\phi\pi^0$ decay in E852 data

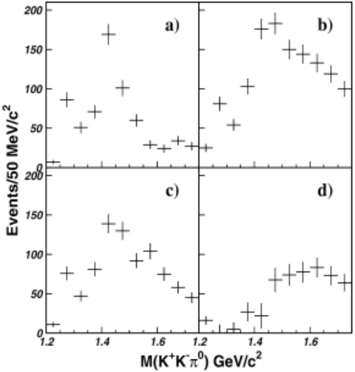

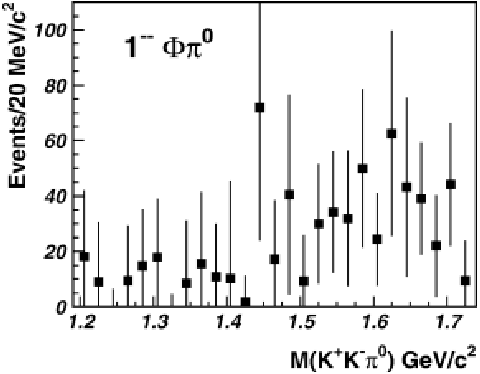

E852 analysis

The left figure shows the side-band study divided $K\bar{K}$ mass spectrum divided into three 10 MeV bins from (a) $1.0 - 1.01$ GeV, (b) $1.015 - 1.025$ GeV, and (c) $1.03 - 1.04$ GeV. The background subtraction is shown in (d). The right figure shows the PWA study using $\phi\pi^0$ S and P waves [**E852**].

[1] G.S. Adams *et al.*, Phys. Lett. **B516**, 264 (2001).

PDG and experimental results possible states

Particle	$I^G(J^{PC})$	Decays	Mass (MeV)	Width (MeV)
$b_1(1235)$	$1^+(1^{+-})$	$K^{*\pm}K^{\mp}\dagger$	1229.5 ± 3.2	142 ± 9
$a_1(1260)$	$1^-(1^{++})$	$KK\pi\ \dagger\ /K^*K\dagger$	1230 ± 40	$250 - 600$
$f_2(1270)$	$0^+(2^{++})$	$K^0K^-\pi^+ + c.c.$	1275.5 ± 0.8	$186.7 \pm 2.2/2.5$
$f_1(1285)$	$0^+(1^{++})$	$KK\pi/K^*K\star/a_0(980)\pi(E852)$	1281.9 ± 0.5	22.7 ± 1.1
$\eta(1295)$	$0^+(0^{-+})$	$a_0(980)\pi(E852)$	1294 ± 4	55 ± 5
$\eta(1405)$	$0^+(0^{-+})$	$KK\pi\dagger/K^*K^\dagger/a_0(980)\pi(E852)$	1408.8 ± 1.8	51.0 ± 2.9
$f_1(1420)$	$0^+(1^{++})$	$KK\pi\ddagger/K^*K\ddagger$	1426.4 ± 0.9	54.9 ± 2.6
$\rho(1450)$	$1^+(1^{--})$	$K^*K + c.c.*$	1476 ± 4	85 ± 9
$\eta(1475)$	$0^+(0^{-+})$	$KK\pi\ \dagger\ /K^*K\ \dagger\ /a_0(980)\pi\dagger$	1475 ± 4	90 ± 9
$\eta_2(1645)$	$0^+(2^{-+})$	$KK\pi\dagger/K^*K\dagger$	1617 ± 5	181 ± 11
$\pi_2(1670)$	$1^-(2^{-+})$	$K * K + c.c.$	1672.2 ± 3.0	260 ± 9
$\phi(1680)$	$0^-(1^{--})$	$K^*K + c.c.\ \ddagger\ /K^0_SK\pi\dagger$	1680 ± 20	150 ± 50
$\rho_3(1690)$	$1^+(3^{--})$	$K\bar{K}\pi$	1688.8 ± 2.1	161 ± 10
$\rho(1700)$	$1^+(1^{--})$	$K^*K + c.c.\dagger$	1720 ± 20	250 ± 100
$\pi(1800)$	$1^-(0^{-+})$	$K^*_0(1430)K^-\ \dagger\ /K^*K^-\star$	$1810 \pm 9/11$	$215 \pm 7/8$
$\phi(1850)$	$0^-(3^{--})$	$K^*K + c.c.\dagger$	1854 ± 7	$87 \pm 28/23$
(2170)	$0^-(1^{--})$	$K^{*0}K^{\pm}\pi^{\mp}\star$	2160 ± 80	125 ± 65

If no marker on the decay(s), has defined branching fraction.

$*$ - possibly seen

$\dagger$ - seen

$\ddagger$ - dominant

$\star$ - not seen

Work cited I

[1] *Jefferson lab*, https://www.flickr.com/photos/jeffersonlab/35359547321/in/album-72157641132946535, Accessed 2021.

[2] S. Adhikari et al., "The gluex beamline and detector", Nuclear Instruments and Methods in Physics Research Section A: Accelerators, Spectrometers, Detectors and Associated Equipment **987**, 164807 (2021).

[3] Y. Qiang, "Detector development for jefferson lab's 12gev upgrade", Nuclear Instruments and Methods in Physics Research Section B: Beam Interactions with Materials and Atoms **350**, 71–76 (2015).

[4] Y. Qiang, "Detector development for jefferson lab's 12gev upgrade", Nuclear Instruments and Methods in Physics Research Section B: Beam Interactions with Materials and Atoms **350**, 71–76 (2015).

Work cited II

[5] *Standard model*, Accessed 2021.

[6] M. Cleven, *Systematic study of hadronic molecules in the heavy-quark sector*, 2014.

[7] *Pseudoscalar nonet*, https://commons.wikimedia.org/wiki/File:Meson$_nonet_{-s}pin_0.svg$, Accessed 2021.

[8] *Vector nonet*, https://commons.wikimedia.org/wiki/File:Meson$_nonet_{-s}pin_1.svg$, Accessed 2021.

[9] D. Griffiths, *Introduction to elementary particles*, 2nd (Wiley-VCH, 2010), pp. 1–52, 115–151.

[10] J. J. Dudek et al., "Toward the excited isoscalar meson spectrum from lattice qcd", Physical Review D **88**, 10.1103/physrevd.88.094505 (2013).

Work cited III

[11] A. Bertin et al. (OBELIX), "E / iota decays to K anti-K pi in anti-p p annihilation at rest", Phys. Lett. B **361**, 187–198 (1995).

[12] P. D. Group et al., "Review of Particle Physics", Progress of Theoretical and Experimental Physics **2020**, 083C01, 10.1093/ptep/ptaa104 (2020).

[13] Z. Bai et al. (MARK-III), "Partial wave analysis of J / psi —> gamma K0(s) K+- pi-+", Phys. Rev. Lett. **65**, 2507–2510 (1990).

[14] R. Aaij et al., "Amplitude analysis of b±→±k+k decays", Physical Review Letters **123**, 10.1103/physrevlett.123.231802 (2019).

[15] I. Vorobiev, "Study of resonance formation in the mass region 1400 – 1500 mev through the reaction →ks0k±", AIP Conference Proceedings **892**, 531–532 (2007).

Work cited IV

[16] G. Adams et al., "Observation of pseudoscalar and axial vector resonances in p→k+k0n at 18 gev", Physics Letters B **516**, 264–272 (2001).

[17] T. Gutsche et al., "Strong decays of radially excited mesons in a chiral approach", Physical Review D **79**, 10.1103/physrevd.79.014036 (2009).

[18] V. Mathieu et al., "Moments of angular distribution and beam asymmetries in 0 photoproduction at gluex", Physical Review D **100**, 10.1103/physrevd.100.054017 (2019).

Work cited for detector section

[1] F. Barbosa, *et al.*, Nucl. Instrum. Methods **A795**, 376 (2015).

[2] Jefferson Lab, https://www.flickr.com/photos/jeffersonlab/35359547321/in/album-72157641132946535, Accessed
2021.

[3] AIP Conference Proceedings **1175**, 020001 (2016).

[4] M. Dugger *et al.*, Nucl. Instrum. Methods **A867**, 115 (2017).

[5] Y. Qiang *et al.* (SOLID), Nucl. Instrum. Methods **B350**, 71 (2015).

[6] M. Albrow *et al.*, Workshop on Physics with Neutral Kaon Beam at JLab (KL2016) Mini-Proceedings, (2016).

[7] S. Adhikari *et al.* (GlueX), Nucl. Instrum. Methods **A987**, 164807 (2021).

[8] N. Jarvis *et al.* (GlueX), Nucl. Instrum. Methods **A962**, 163727 (2020).

[9] T. Beattie *et al.* (GlueX), Nucl. Instrum. Methods **A896**, 24 (2018).

[10] E. Pooser *et al.* (GlueX), Nucl. Instrum. Methods **A927**, 330 (2019).